



REPORT

Environmental controls on daytime net community calcification on a Red Sea reef flat

W. N. Bernstein^{1,2}  · K. A. Huguen³ · C. Langdon⁴ ·
D. C. McCorkle³ · S. J. Lentz³Received: 8 July 2015 / Accepted: 29 December 2015 / Published online: 23 January 2016
© Springer-Verlag Berlin Heidelberg 2016

Abstract Coral growth and carbonate accumulation form the foundation of the coral reef ecosystem. Changes in environmental conditions due to coastal development, climate change, and ocean acidification may pose a threat to net carbonate production in the near future. Controlled laboratory studies demonstrate that calcification by corals and coralline algae is sensitive to changes in aragonite saturation state (Ω_a), as well as temperature, light, and nutrition. Studies also show that the dissolution rate of carbonate substrates is impacted by changes in carbonate chemistry. The sensitivity of coral reefs to these parameters must be confirmed and quantified in the natural environment in order to predict how coral reefs will respond to local and global changes, particularly ocean acidification. We estimated the daytime hourly net community metabolic rates, both net community

calcification (NCC) and net community productivity (NCP), at Sheltered Reef, an offshore platform reef in the central Red Sea. Average NCC was $8 \pm 3 \text{ mmol m}^{-2} \text{ h}^{-1}$ in December 2010 and $11 \pm 1 \text{ mmol m}^{-2} \text{ h}^{-1}$ in May 2011, and NCP was $21 \pm 7 \text{ mmol m}^{-2} \text{ h}^{-1}$ in December 2010 and $44 \pm 4 \text{ mmol m}^{-2} \text{ h}^{-1}$ in May 2011. We also monitored a suite of physical and chemical properties to help relate the rates at Sheltered Reef to published rates from other sites. While previous research shows that short-term field studies investigating the NCC– Ω_a relationship have differing results due to confounding factors, it is important to continue estimating NCC in different places, seasons, and years, in order to monitor changes in NCC versus Ω in space and time, and to ultimately resolve a broader understanding of this relationship.

Communicated by Biology Editor Dr. Anastazia Banaszak

Electronic supplementary material The online version of this article (doi:[10.1007/s00338-015-1396-6](https://doi.org/10.1007/s00338-015-1396-6)) contains supplementary material, which is available to authorized users.

✉ W. N. Bernstein
whitney.bernstein@gmail.com

¹ MIT-WHOI Joint Program in Oceanography/Applied Ocean Science Engineering, Department of Marine Chemistry and Geochemistry, Woods Hole Oceanographic Institution (WHOI), 266 Woods Hole Road, Woods Hole, MA 02543, USA

² Massachusetts Institute of Technology (MIT), Cambridge, MA, USA

³ Department of Marine Chemistry and Geochemistry, Woods Hole Oceanographic Institution (WHOI), 266 Woods Hole Road, Woods Hole, MA 02543, USA

⁴ University of Miami Rosenstiel School of Marine and Atmospheric Science, Miami, FL, USA

Keywords Coral · Calcification · CaCO_3 · Acidification · Aragonite saturation

Introduction

Biologically mediated calcification is an essential process on coral reefs. Corals build the foundation of the reef, enabling the reef to keep pace with changes in local sea level (Stoddart 1969; Grigg 1982; Kleypas and Langdon 2006; Kleypas et al. 2006). Coralline algae, foraminifera and sand serve as the infill and cement that fortify the reef foundation (Adey 1998; Kleypas and Langdon 2006; Kleypas et al. 2006). Coral colonies of diverse morphologies create the complex habitat that supports the extremely high biodiversity of reef ecosystems (Kleypas and Langdon 2006; Kleypas et al. 2006). Net community calcification (NCC) is the production of biogenic carbonate minerals by calcifying organisms minus the loss of that material by dissolution.

The growth of calcifying reef organisms is presently threatened by environmental changes due to climate change and ocean acidification (Kleypas et al. 2006; Pandolfi et al. 2011), in addition to the local stresses imposed by coastal development, harmful fishing practices, invasive species, and disease.

Ocean acidification (OA) is the process by which anthropogenic CO₂ dissolves in the surface ocean and depresses the pH and carbonate saturation state (Ω) of seawater. Results from controlled experiments and field studies indicate that a decline in aragonite saturation state (Ω_a) reduces coral and algal calcification rates and increases dissolution rates of carbonate sediments and reef matrix (Marubini and Atkinson 1999; Langdon et al. 2000; Leclercq et al. 2000; Marubini et al. 2001; Langdon and Atkinson 2005; Jokiel et al. 2008; Kuffner et al. 2008; Martin and Gattuso 2009). The combined effect of reduced calcification rates and increased dissolution rates is reduced NCC. The negative impact on calcification rates is presumably because the biologically mediated precipitation of a given mineral is more energetically costly when the mineral saturation state and pH of the seawater are depressed. Corals have been shown to mediate calcification by regulating the saturation state and pH of the internal fluid from which the carbonate skeleton precipitates (Venn et al. 2011, 2013; McCulloch et al. 2012). Experiments have established that calcification in hermatypic scleractinian corals is enhanced by light (Wainwright 1963; Chalker and Taylor 1975; Barnes 1982; Gattuso et al. 1999; Marubini et al. 2001; Allemand et al. 2004; Muscatine et al. 2005) and photosynthesis (Goreau and Goreau 1959; Gattuso et al. 1999; Allemand et al. 2004). This may confound the NCC– Ω_a relationship observed in the field. Recent experiments have suggested that nutrient uptake and heterotrophic feeding also impact calcification rates (Marubini and Davies 1996; Houlbreque et al. 2003) and may in fact decrease the sensitivity of calcification to Ω_a (Langdon and Atkinson 2005; Silverman et al. 2007a, b; Cohen and Holcomb 2009). Although the mechanistic links between light, nutrition and calcification are not yet fully understood, it is clear that the impacts of multiple environmental factors on both calcification and dissolution must be considered when investigating the impact of OA on NCC in an observation-based field study.

While mesocosm studies have demonstrated that NCC is sensitive to changes in Ω_a , confirming this dependence in the natural environment is challenging. The large differences in the correlations observed at different sites has highlighted the need for a deeper understanding of environmental controls on metabolic rates at various timescales before extrapolating correlations globally or over several decades (Pandolfi et al. 2011; Shamberger et al. 2011; Andersson and Gledhill 2013). Each empirical NCC– Ω_a

correlation is influenced by several factors including the relative rates of NCC and net community production (NCP) (Andersson and Gledhill 2013) and contemporaneously variable temperature, light, and nutrition (or feeding) levels. The relationship determined for short-term local studies can also be affected by the fluctuating residence time of the water. For example, water that is exposed to a certain NCC or NCP for a long time will exhibit lower Ω than water exposed to that same NCC or NCP for a shorter period of time (Shaw et al. 2012; Zhang et al. 2012; Falter et al. 2013; McMahan et al. 2013). In order to gain a predictive understanding of how coral reefs worldwide will respond to OA, we must investigate the relationships between metabolic rates and environmental conditions in diverse regions, reef settings (e.g., fringing reef or outer shelf reef), and reef zones (e.g., fore-reef, reef flat, lagoon) (Kleypas and Langdon 2006; Atkinson and Cuet 2008).

In this study we estimated NCC and NCP rates on Sheltered Reef, a platform reef on the mid-shelf of the Red Sea near Jeddah, Saudi Arabia. The goal of this study was to examine the relationship between NCC and NCP and the physiochemical environment on an hourly timescale and to compare the results with those from previously published studies in the Red Sea and other regions. A study of NCC in the Red Sea is of particular interest in comparison with similar studies elsewhere, because the Red Sea has relatively high temperature (mean global sea temperature is 27.6 °C, mean for this study was 29 ± 0.9 °C) and Ω_a (mean global Ω_a is 3.8, mean for this study was 4.6 ± 0.1) (Kleypas et al. 1999, Silverman et al. 2007b).

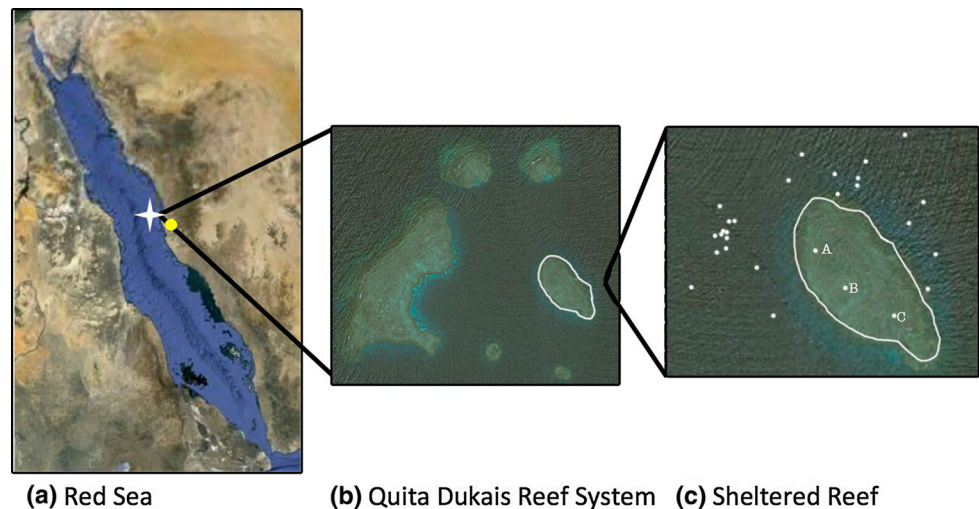
Methods

Study site

Our study reef is a small (275×125 m²) platform reef within the Quita Dukais offshore reef platform in the eastern Red Sea, north of Jeddah (21°59'N, 38°51'E, Fig. 1). We named it Sheltered Reef (SR) because it is on the leeward side of a larger reef. Samples were collected on 7 and 8 December 2010, and 21–23 May 2011. The temperature around Quita Dukais ranges from 25 °C in February to 31 °C in August and is about 28 °C in both December and May (Fig. 2). Light levels are at a minimum in December and reach a maximum in May (Fig. 2). The water is oligotrophic (Table 1).

SR has rich coral cover on the steep walls and rim. The reef flat is about 1 m deep (Fig. 3) with maximum tidal range of approximately 30 cm and hosts a community consisting of 41 % rhodoliths (free-living coralline algal crusts; Foster 2001; Donnan and Moore 2003; Fig. 4b), 28 % algal turf (non-calcifying algae), 15 % crustose

Fig. 1 Sheltered Reef (21°59'N, 38°51'E), a small (275 × 125 m²) offshore platform reef within the Quita Dukais reef system [white star in (a), also shown in (b)], in the central Red Sea, near Jeddah [yellow circle in (a)]. Open ocean samples were collected from locations marked with unlabeled white points (c). Reef flat samples were collected at the three points (A, B and C). Images from Google Earth



coralline algae, 8 % sand, and 5 % live coral (Fig. 4a). The corals present are mainly *Stylophora* spp., *Porites* spp., and *Platygyra* spp.

SR is a particularly interesting site because the community is largely composed of coralline algae, in both rhodolith and encrusting forms. This group of calcifying organisms fulfills many important functional roles in coral reef systems. A rhodolith bed is a complex three-dimensional matrix that provides habitat for numerous associated invertebrates and macroalgae (Foster 2001; Donnan and Moore 2003). Crustose coralline red algae serve as a settling cue for juvenile coral recruits (Morse et al. 1994; Birrell et al. 2008). Crustose coralline algae also cement and consolidate the reef foundation, supporting the con-

struction of diverse habitats, guarding against erosion, and in some cases serving as the principal driver of carbonate accumulation on reefs (Bjork et al. 1995). Coralline algae may be more susceptible to ocean acidification than coral with aragonite skeletons because they are made of high-magnesium calcite (HMC), and biogenic HMC is typically a more soluble carbonate mineral than aragonite (Bischoff et al. 1987; Morse et al. 2006; Anthony et al. 2008; Jokiel et al. 2008; Kuffner et al. 2008; Martin and Gattuso 2009). This study is one of few that have examined calcification in natural communities dominated by coralline algae (Chisholm 2000).

Determination of metabolic rates

We estimated daytime NCC and NCP rates at SR using an Eulerian flow respirometry method (Odum 1956; Langdon et al. 2010), in which we compared the alkalinity and dissolved inorganic carbon (DIC) concentration of the upstream open ocean end-member (unlabeled white points, Fig. 1) and the reef flat end-member (points A, B, and C, Fig. 1). We used the changes in salinity-normalized¹ alkalinity and salinity-normalized DIC together with estimates of current speeds and reef geometry to calculate

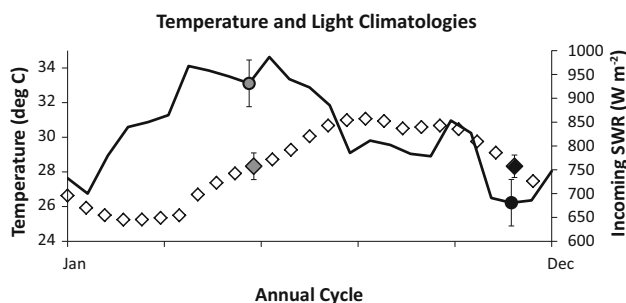


Fig. 2 The light climatology (black line) shows monthly average mid-day (between 1100 and 1300 h) flux of incoming short wave radiation (SWR, W m⁻²) and is based on data from the meteorological tower located at King Abdullah University of Science and Technology, November 2009 to March 2012. The temperature climatology (diamonds, °C) is based on Advanced Very High-Resolution Radiometer (AVHRR, v5, 4-km grid size) sea surface temperature data from 1985 to 2009. Gray symbols represent values for May and black symbols represent values for December. Error bars are standard deviations

¹ Normalization to constant salinity (Normalized Alkalinity = Alkalinity × 40/Salinity) removes the effects of evaporation and precipitation on alkalinity and DIC. This should not make a large difference in most reef settings, but we chose to do this because we were confident in our salinity measurements (accuracy = 0.001 PSU, resolution 0.0002 PSU), so there was little danger of confounding the results with faulty salinity measurements.

Table 1 Maximum and minimum levels in incoming short wave radiation (PAR, $\mu\text{E m}^{-2} \text{s}^{-1}$)^a in December and May. Nitrate and phosphate concentrations (μM), temperature ($^{\circ}\text{C}$), aragonite saturation state (Ω_a^a), partial pressure of CO_2 ($p\text{CO}_2$, μatm)^a and pH^a were

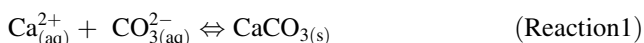
	<i>n</i>	Temperature $^{\circ}\text{C}$	Ω_a^a	$p\text{CO}_2^a$ μatm	pH^a	PAR ^b $\mu\text{E m}^{-2} \text{s}^{-1}$	$[\text{NO}_3]$ μM	$[\text{PO}_4]$ μM	NCC $\text{mmol m}^{-2} \text{h}^{-1}$	NCP $\text{mmol m}^{-2} \text{h}^{-1}$
December	12	29.6 ± 0.3	4.6 ± 0.3	340 ± 50	8.10 ± 0.05	1350 ± 130	0.2 ± 0.1	0.04 ± 0.03	8 ± 3	21 ± 7
May	42	28.4 ± 0.6	4.5 ± 0.3	340 ± 40	8.10 ± 0.03	1530 ± 660	0.2 ± 0.2	0.1 ± 0.03	11 ± 1	44 ± 4
Average of December and May	2	29.0 ± 0.9	4.6 ± 0.1	340 ± 2	8.10 ± 0.00	1440 ± 130	0.2 ± 0.0	0.07 ± 0.04	9 ± 2	33 ± 12

^a Calculated from alkalinity and DIC using the CO2SYS program (Pierrot and Wallace 2006), applying the total pH scale (mol kg^{-1} sea water), the carbonate species dissociation constants of Mehrbach et al. (1973) as refit by Dickson and Millero (1987), and the aragonite solubility constant of Mucci (1983)

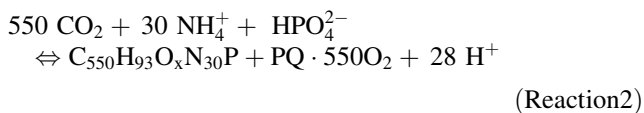
^b Average of short wave radiation flux was integrated over 1100–1300 h on the three sampling days. The flux of PAR is estimated as 43 % of total incoming radiative energy flux (Baker and Frouin 1987) which is divided by 0.21 (Onsetcomp.com) to convert W m^{-2} to $\mu\text{E m}^{-2} \text{s}^{-1}$

NCC and NCP rates, respectively. By budgeting these two parameters, we are able to estimate the net metabolic rates.

The two reactions of interest are calcification and photosynthesis. Calcification results in the loss of two equivalents of alkalinity and one mole of DIC for each mole of CaCO_3 produced:



In contrast, photosynthesis results in a decrease in DIC by one mole and a negligible change in alkalinity [$\Delta\text{ALK}:\Delta\text{DIC} = 28:550$, for photosynthesis on coral reefs (Atkinson and Smith 1983; Atkinson and Falter 2003)] for each mole of organic carbon produced:



where PQ is photosynthetic quotient or the moles of O_2 produced for each mole of CO_2 assimilated.

Therefore, the budget for alkalinity describes NCC:

$$\text{NCC} = 0.5\rho_w h \frac{\Delta A_T}{\Delta t} - 0.5\rho_w u h \frac{\Delta A_T}{L} \quad (1)$$

where NCC is the instantaneous net calcification rate ($\text{mmol m}^{-2} \text{h}^{-1}$). NCC is the sum of the rate of change of the total alkalinity (A_T) inventory along the transect plus the advective flux of A_T into and out of the transect, assuming the diffusive flux is small (Falter et al. 2008). $\Delta A_{L/T}$ is the change in alkalinity from the open ocean to the reef flat ($A_{\text{reef}} - A_{\text{open ocean}}$) along the length (m) of reef substrate over which the water passes, L . $\Delta A_T/\Delta t$ is the rate of change in average (reef and open ocean) alkalinity as measured between subsequent transects. ρ_w is the density of seawater ($\sim 1026 \text{ kg m}^{-3}$), u is the speed of the water (m h^{-1}), averaged both vertically and over the 4-min duration of each hourly velocity measurement, and h is the depth (m) of the water on top of the reef.

similar on the reef flat in December and May. Values listed as mean \pm standard deviation, except net community calcification (NCC) and net community productivity (NCP) values ($\text{mmol m}^{-2} \text{h}^{-1}$) listed with standard error

The budget for DIC incorporates the effects of NCP and NCC and gas exchange on DIC:

$$\text{NCP} = \rho_w h \frac{[\Delta\text{DIC} - 0.5\Delta A_T]}{\Delta t} - \rho_w u h \frac{[\Delta\text{DIC} - 0.5\Delta A_T]}{L} + F_{\text{ASGE}} \quad (2)$$

where NCP is the instantaneous net productivity ($\text{mmol m}^{-2} \text{h}^{-1}$). Again, we have assumed that the diffusive flux is small (Falter et al. 2008). The terms in Eq. 2 are analogous to those in Eq. 1, except the change in DIC is corrected by $0.5\Delta A_T$ to account for the change in DIC that derives from the calcification process (Reaction 1). F_{ASGE} is the flux of carbon due to the air–sea gas exchange of CO_2 . However, because CO_2 equilibrates slowly with the atmosphere this term is negligible ($<0.35 \text{ mmol m}^{-2} \text{h}^{-1}$) (Wanninkhof 1992; Frankignoulle et al. 1996; Sweeney et al. 2007) and is not included in the calculation.

The uncertainty for NCC and NCP is calculated using the differential method (the relative error is the square root of the sum of the squares of the relative errors) to propagate the uncertainty of all input parameters, ΔA_T , ΔDIC , u , h , L , addressed individually below. This uncertainty for both NCC and NCP is about 24 % [$2 \text{ mmol m}^{-2} \text{h}^{-1}$ for NCC and $12 \text{ mmol m}^{-2} \text{h}^{-1}$ for NCP (Table 1)]. The values estimated by this method represent an average over an appreciable area due to lateral mixing of reef waters (Kinsey 1985).

Sample collection and analysis

Water samples for determination of DIC, alkalinity, salinity, and nutrients were collected from the reef–water interface using a hand-held Niskin sampler. We measured DIC and alkalinity using a Marianda VINDTA-3C analysis system, in Dr. Daniel McCorkle’s lab at Woods Hole Oceanographic Institution (WHOI). Alkalinity was

determined by nonlinear curve-fitting to data obtained by open-cell titrations, and DIC concentrations were determined by coulometric analysis. Both measurements were standardized using certified reference materials obtained from Dr. A. Dickson at the Scripps Institution of Oceanography. The analytical precision for alkalinity based on replicate samples was $1.2 \mu\text{mol kg}^{-1}$ ($n = 90$ pairs), and for DIC was $3.4 \mu\text{mol kg}^{-1}$ ($n = 90$ pairs). Salinity was measured using a Guildline salinometer at WHOI (accuracy = 0.001 PSU, resolution 0.0002 PSU; D. Wellwood, pers. comm., March 2013).

We sampled the open ocean end-member from the waters surrounding the reef (unlabeled white points in Fig. 1c) in the morning and afternoon of each day. We evaluated spatial variability in the open ocean end-member by collecting water from 1-m depth at three different locations within the open ocean region on each morning of three consecutive days in December. The variability between these locations for alkalinity and DIC was less than the analytical precision of the measurement (Electronic Supplementary Material, ESM, Table S1). Therefore, although we always aimed to sample upstream of the reef each morning and afternoon, we assumed the open ocean end-member to be uniform in space.

We sampled on the reef flat at three points along the long axis of the reef (points A, B, C in Fig. 1c) twice per day for 2 d in December, and four to five times per day for 3 d in May. To calculate NCC and NCP, we compared the reef flat values to the open ocean values that corresponded most closely to the sampling time of each reef flat end-member. This yielded two to five NCC and NCP estimates at each point each day. Samples were collected between 0900 and 1600 h, during peak sunlight hours.

Input parameters

The calculations of NCC and NCP require input of the water velocity (u), water depth (h), and the distance (L) over which the water traveled over the reef flat. A 2 MHz Nortek Aquadopp Profiler, located at point B (Fig. 1c), sampled the current profile for 4 min at hourly intervals with 2.5 cm vertical resolution, and 1 s temporal resolution. This sampling program was designed for a separate year-long study, and the data were generously provided to us by our colleagues, Drs. Steve Lentz and James Churchill. We understand that this sampling resolution was not ideal for our study and may have introduced aliasing problems. When determining cross-reef transport, we based the calculation on the linear interpolation between sampling bursts. The depth-averaged Stokes drift (wave transport) was negligible in May ($\sim 0.1 \text{ cm s}^{-1}$) and only 0.3–1 cm s^{-1} in December (S. Lentz, pers. comm. June 2013); therefore, Stokes drift was not included in

calculations of cross-reef transport, and is a source of additional uncertainty for the four points in December. Because the water was shallow ($\sim 1 \text{ m}$) and the benthic topography was rough, we assumed that the water column was well mixed, and we used the vertically integrated water velocity (analytical error 0.1 cm s^{-1}).

The changes in depth were measured using a Seagauge Wave and Tide Recorder (SBE 26 plus). The Seagauge was located at the northern end of the reef, so the raw data were corrected by $21 \pm 5 \text{ cm}$ to account for the depth of the Aquadopp relative to the Seagauge. We used the water depth and water velocity at the Aquadopp because the product of depth and velocity is equal everywhere on the reef flat when flow is non-divergent and non-convergent.

The distance, L , was estimated as the length from the sampling point to the reef edge, following the direction of flow at the sampling time. The reef edge was defined by a GPS track generated by swimming the perimeter of the reef with a hand-held GPS unit (white loop in Fig. 1, black loops in Fig. 5). The distance was calculated from each sampling point to the edge of the reef following the direction of flow described by the velocity measurements. The error in distance was estimated as the difference between subsequent estimates. We estimated a minimum error of 5 m to account for uncertainties in our knowledge of the exact positions along the reef edge and positions at points A, B, and C. An additional source of uncertainty arises from the fact that a given parcel of water may follow a meandering path and may experience changes in speed as it moves across the reef. However, because we did not follow a parcel of water, we were compelled to make the simplest assumption that the water followed a linear path across the reef (Fig. 5). Using the assumption of linear flow yields a minimum estimate of L , a maximum estimate of metabolic rate.

Environmental parameters

Ω_a , temperature, light, and nutrient (ammonium, nitrate, nitrite) concentrations all influence NCC and NCP (Kleypas and Langdon 2006; Kleypas et al. 2006). In addition, nitrogen fixation and consumption of dissolved and particulate organic matter can also be important sources of nutrition for reef communities (Kinsey 1985; Erez 1990; Ribes et al. 2003). Inorganic nutrient concentrations were measured at Oregon State University using a continuous segmented flow system consisting of a Technicon AutoAnalyzer II (SEAL Analytical) and an Alpkem RFA 300 Rapid Flow Analyzer (Alpkem), as described in Apprill and Rappe (2011). The precisions for nitrite and nitrate + nitrite were 0.02 and 0.15 μM , respectively.

Ω_a was calculated from the measured alkalinity, DIC, temperature, and salinity. Although the reef in this study is

Table 2 Instantaneous net community calcification (NCC) and net community productivity (NCP) at Sheltered Reef in December 2010 and May 2011 ($\text{mmol m}^{-2} \text{h}^{-1}$)

Date	Time	Color Code	Point	NCC	se	NCP	se	Ω	Temp	PAR
				$\text{mmol m}^{-2} \text{h}^{-1}$		$\text{mmol m}^{-2} \text{h}^{-1}$		$^{\circ}\text{C}$		$\mu\text{E m}^{-2} \text{s}^{-1}$
7-Dec-10	11:50	Yellow	A	13	6	23	11	5.1	29.9	1193
	12:37		B	3	2	12	12	4.5	29.7	
	13:25	Blue	C	2	5	10	5	4.3	29.5	
8-Dec-10	11:45	Yellow	A	4	1	12	5	4.7	29.8	1359
	12:27		B	19	3	53	15	4.7	29.5	
	13:10	Blue	C	4	1	17	3	4.2	29.4	
21-May-11	10:20	Red	A	5.1	0.1	16.2	0.2	4.4	27.9	1652
	10:50		B	19	3	49	8	4.6	28.2	
	11:20	Yellow	C	13	4	47	10	4.4	27.8	
	11:50	Green	A	13	4	52	21	4.4	28.1	
	12:20		B	9	2	36	9	4.7	28.5	
	12:50	Green	C	23	11	64	27	4.8	28.6	
	13:20	Blue	A	19	1	68	2	4.5	28.3	
22-May-11	10:20	Red	B	17	3	61	4	4.7	28.6	834
	10:50		C	15	4	65	8	4.9	29.1	
	11:20	Yellow	A	7	1	24	17	4.1	27.6	
	11:52		B	8	1	14	8	4.1	27.6	
	12:25	Green	C	7	2	23	17	4.1	27.6	
	13:05		A	6.6	0.4	45	16	4.3	27.8	
	13:45	Blue	B	6	1	32	14	4.2	27.8	
	14:17		C	5	1	39	7	4.2	27.8	
	14:50	Purple	A	12	4	69	9	4.3	28.0	
			B	11	4	58	13	4.3	28.0	
23-May-11	10:00	Red	C	9	4	66	13	4.3	28.0	983
	10:35		A	13	2	70	2	4.4	28.0	
	11:10	Yellow	B	17	3	72	3	4.5	28.2	
	11:52		C	16	1	67	10	4.4	28.2	
	12:35	Green	A	13	2	48	4	4.6	28.6	
	13:10		B	17	3	60	15	4.7	28.9	
	13:45	Blue	C	2.11	0.2	22	5	4.2	28.5	
	14:15		A	3	3	13	9	4.6	28.7	
	14:45	Purple	B	12	4	44	16	4.9	29.0	
			C	16	4	63	5	4.7	29.0	
			A	6	2	22	9	4.4	28.5	
			B	-2.1	0.1	1	2	4.7	28.8	
			C	0.89	0.04	10	3	5.0	29.6	
			A	10	2	46	10	4.4	28.6	
			B	12	3	43	9	4.5	28.8	
			C	16	7	68	31	4.9	29.3	

'se' is standard analytical error. Colors correspond to the approximate times of sampling transects in Fig. 5. Actual transect times are indicated in gray. Sequential transects were averaged when adding the advection and time-dependent terms, resulting in a new time assignment as indicated in black and illustrated by each data set straddling the color bars for each transect. Aragonite saturation state (Ω), temperature (Temp $^{\circ}\text{C}$) and photosynthetically available radiation (PAR, $\mu\text{E m}^{-2} \text{s}^{-1}$) are also listed

The advection terms for NCC and NCP at point A at 1325 h on 7 December are more than four standard deviations above the means (60 and $177 \text{ mmol m}^{-2} \text{h}^{-1}$, respectively). The advection data are non-normally distributed with these outliers included, but distributions are normal when these outliers are excluded. The lowest NCC advection value ($-5 \text{ mmol m}^{-2} \text{h}^{-1}$) also occurs at the same time, but at point C. By conditional logic it is unlikely for this to randomly occur on the exact same date and time as the anomalously highest value. Also, it is unlikely that such a high rate of net dissolution would occur in the very middle of the day when all of the other data from all other times exhibit positive net calcification. For these reasons, we suspect something was amiss with the sample at point C of the second transect on 7 December, and excluded this value as well. The text describes results excluding the two outliers for advection terms for NCC and the single outlier for NCP

primarily composed of coralline algae that produce HMC, we calculated Ω with respect to aragonite because studies have found that biogenic Mg calcites exhibit a wide range of solubilities even for Mg calcites of similar Mg content (Morse et al. 2006). Therefore, we used Ω_a , which is most relevant to the previously published literature. The calculation was carried out using the CO2SYS program (Pierrot and Wallace 2006), applying the carbonate species dissociation constants of Mehrbach et al. (1973) as refit by Dickson and Millero (1987), and the aragonite solubility constant of Mucci (1983). The values of Ω_a reported here can be multiplied by a factor of 0.8–1.0 to approximate Ω_{HMC} (Morse et al. 2006).

Temperature was measured using several tools, including a YSI sonde; a conductivity, temperature, depth (CTD) logger; and numerous Hobo temperature loggers. Incoming short wave radiation (SWR) was measured in W m^{-2} at a meteorological tower located 43 km away on the campus of King Abdullah University of Science and Technology (22°17.823'N, 39°05.567'E).

Results

Measurements

The average photosynthetically active radiation (PAR) from 1100 to 1300 h was $1350 \pm 130 \text{ W m}^{-2}$ in December and $1530 \pm 660 \text{ W m}^{-2}$ in May (mean \pm SD) (Table 1). The measured reef flat temperatures were approximately 29 °C on the sampling days in both seasons (Table 1), and the salinity was approximately 39 PSU. The average reef flat Ω_a was approximately 4.6 in both seasons (Table 1).

Average nitrate and phosphate concentrations were 0.2 ± 0.0 and $0.07 \pm 0.04 \mu\text{M}$ (mean \pm SD), respectively ($n = 2$ seasons, see Table 1 for seasonal averages). These values are typical of coral reef systems worldwide (nitrate typical range: 0.05–0.5 μM , phosphate typical range: 0.05–0.3 μM ; Atkinson and Falter 2003).

The input parameters for calculating NCC and NCP were water depth, current speed, and length of reef substrate traversed. Average water depth was just under 1 m (Fig. 3). The water speed ranged from 0 to 6 cm s^{-1} and was highly variable (Fig. 3). The lengths of reef over which the water passed ranged from 20 to 200 m (Fig. 5).

NCC and NCP

Daytime hourly NCC and NCP were estimated at three points on the reef flat (Fig. 1c, points A, B, C) during each season. The daytime NCC rates ranged from 2 to 19 $\text{mmol m}^{-2} \text{h}^{-1}$ in December and from -2 to 23 $\text{mmol m}^{-2} \text{h}^{-1}$ in May (Table 2). The daytime NCP rates ranged from 10 to

53 $\text{mmol m}^{-2} \text{h}^{-1}$ in December and from 1 to 72 $\text{mmol m}^{-2} \text{h}^{-1}$ in May (Table 2). The average daytime NCC for the reef was $8 \pm 3 \text{ mmol m}^{-2} \text{h}^{-1}$ in December and $11 \pm 1 \text{ mmol m}^{-2} \text{h}^{-1}$ in May (Table 1). Integrating over 12-h days and assuming nighttime NCC around zero (Yates and Halley 2003; Shamberger et al. 2011; Albright et al. 2013), this equates to NCC of 91 $\text{mmol m}^{-2} \text{d}^{-1}$ in December and 129 $\text{mmol m}^{-2} \text{d}^{-1}$ in May. These values are within the range of previously published studies (Table 3; ESM Table S2), and at the extremes of the range ($110 \pm 19 \text{ mmol m}^{-2} \text{d}^{-1}$) of the long-term “standard performance” for coral/algal flats between 23°S and 21°N (Kinsey 1983).

The average daytime NCP for the reef was $21 \pm 7 \text{ mmol m}^{-2} \text{h}^{-1}$ in December and $44 \pm 4 \text{ mmol m}^{-2} \text{h}^{-1}$ (mean \pm SE) in May (Table 1). These are within the range observed in previously published studies (Table 3; ESM Table S2).

Regressions

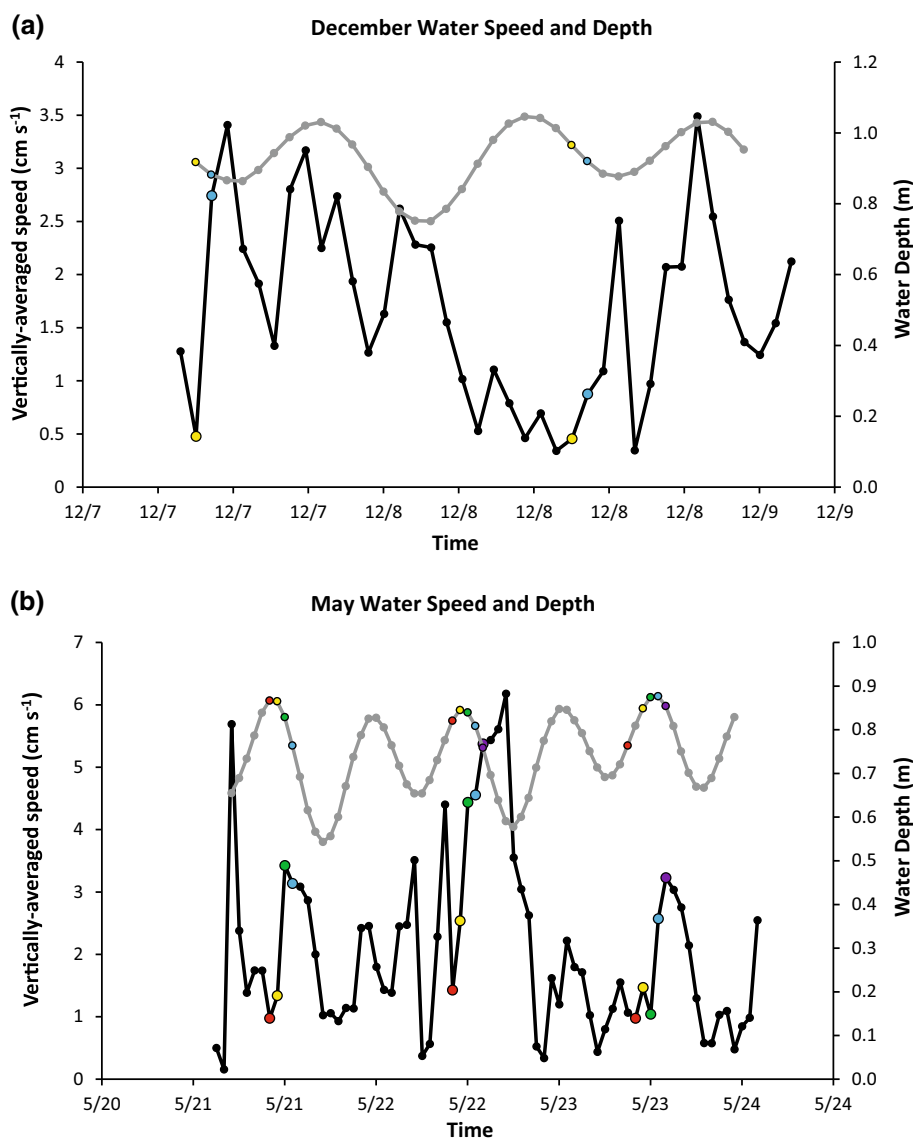
NCC was strongly correlated with NCP ($r^2 = 0.71$, $p < 0.0001$; Table 4; Fig. 6). The correlation between NCC and Ω_a was also significant ($p = 0.05$; Fig. 7; Table 4). However, the variance explained was low due to the large scatter ($r^2 = 0.1$; Table 4). Both NCC and NCP showed a weak but significant correlation with nitrate concentration (Fig. 8). Regressions of both NCC and NCP against light and temperature were weak and insignificant (Table 4).

Discussion

Seasonal differences

Both NCC and NCP were higher in May (11 ± 1 and $44 \pm 4 \text{ mmol m}^{-2} \text{h}^{-1}$, respectively) than in December (8 ± 3 and $21 \pm 7 \text{ mmol m}^{-2} \text{h}^{-1}$, respectively). While temperature, nutrient concentrations, and Ω_a showed similar values in both December and May (Table 1), seasonally averaged light showed a larger difference between the seasons (Table 1; Fig. 2) and is a plausible driver of the difference in NCC and NCP between the sampling seasons. It is plausible that temperature is also a driver of metabolic variability on seasonal timescales, but we were not able to test this because the maximum variability in temperature did not coincide with our sampling seasons (Fig. 2). Long-term studies with higher-resolution (i.e., weekly or monthly) sampling to capture the full intra- and inter-seasonal variability would be required to quantify the relationships between metabolic rates and light, temperature, and nutrient concentrations on a seasonal timescale.

Fig. 3 Depth (gray) and vertically averaged water speed (black) in December (a) and May (b) at Sheltered Reef. The colors indicate time of day for water samples and resulting flux estimates: 1000–1100 h (red), 1100–1200 h (yellow), 1200–1300 h (green), 1300–1400 h (blue), 1400–1500 h (purple)



Comparison with previously published data

The NCC and NCP values obtained for SR are within the range of values obtained for coral reefs worldwide (Table 3; ESM Table S2). The range in average daytime metabolic rates reported over the past three decades appears to be quite large (0–18 mmol m⁻² h⁻¹ for NCC, and –2 to 100 mmol m⁻² h⁻¹ for NCP). This large range may be due to differences in Ω_a or community structure (including calcifying organism, sediments, carbonate framework, and the organisms involved in dissolution) and

indeed, when comparing metabolic rates at different reefs, care must be taken to consider the community composition, environmental conditions, and methods used (Kinsey 1985; Atkinson and Cuet 2008).

NCC– Ω_a relationship and confounding factors

The relationship between NCC and Ω_a is of keen interest because the x-intercept of the relationship represents the threshold Ω_a at which the community transitions from positive to negative net production. A coral reef cannot

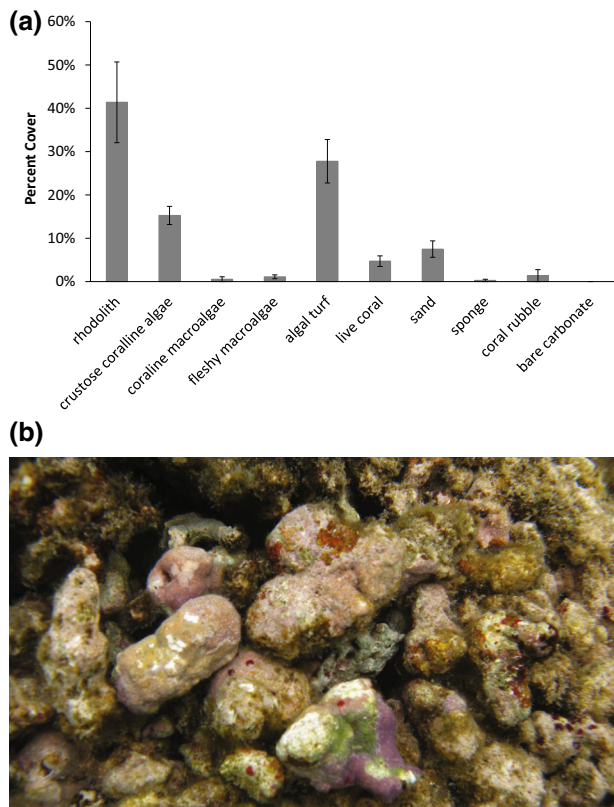


Fig. 4 **a** The community composition at Sheltered Reef, dominated by **b** rhodoliths, a free-living form of coralline algae. Benthic data were collected using the line-intercept method over four randomly placed 50 m transects. Error bars show standard error

persist indefinitely if it is not able to sustain positive net production of calcium carbonate in the long term. Predicting long-term impacts of ocean acidification by extrapolating from short-term studies is problematic for three main reasons. First, the timescale of observation (hourly, daily) is typically very short relative to the time scale for which predictions are needed (annual to decadal). Thus, one must recognize the implicit assumption in basing long-term predictions on short-term observations that the relationship between NCC and Ω_a is the same on both short and long timescales (Langdon et al. 2000). Second, the range of Ω_a values encountered in a short-term study is likely to be very small and not extend to the values that are predicted for the end of the century (Silverman et al. 2007b, 2012; Shamberger et al. 2011; Albright et al. 2013) (the exception is very shallow sites; Shaw et al. 2012). This means that if the relationship over the broader range is not linear or even if the relationship is linear but the relationship is poorly constrained the uncertainty in the extrapolated x-intercept (threshold Ω_a where $NCC = 0$) will be unacceptably large. The third problem is that some factors that affect NCC co-vary with Ω_a (i.e., light, temperature, nutrients, NCP) (Falter et al. 2012). This means that if

these factors positively influence NCC, then plotting NCC against Ω_a will lead to the false conclusion that too much of the change in NCC is explained by Ω_a (i.e., the slope of the NCC– Ω_a relationship will be overestimated; Venti et al. 2014). In contrast, if the co-varying factor has a negative effect on NCC the plot of NCC against Ω_a will underestimate the true slope of the NCC– Ω_a relationship. Increasing the duration of field studies, improving the precision of the NCC measurements, and measuring a suite of environmental parameters (temperature, light, NCP, community composition, etc.) will be necessary to address these issues.

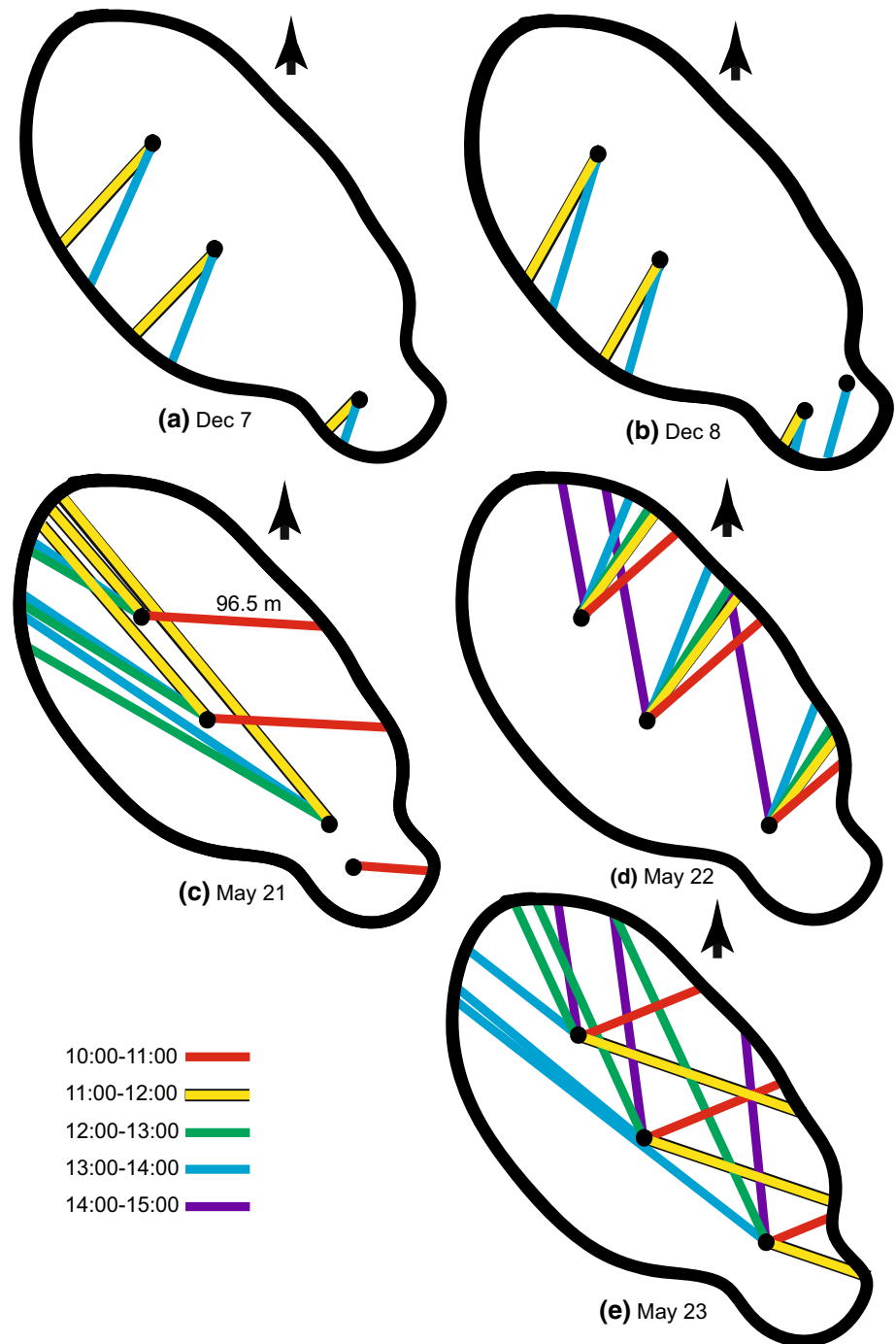
NCC– Ω_a relationship compared to previously published studies

In this study, Ω_a where $NCC = 0$ (intercept) was 3.1 ± 2.7 (SE) (Table 5). This parameter has been found to vary widely between studies from a low of 1.2 ± 1.6 (Shaw et al. 2012) to a high of 4.9 ± 0.3 (Ohde and van Woesik 1999). The mean of this parameter for all field studies is 2.9 ± 0.5 (SE) (Table 5). It is interesting that the x-intercept from mesocosm studies is significantly lower, 1.2 ± 0.2 (Table 5).

The broad range in Ω_a at which $NCC = 0$ might be explained by differences in dissolution rates between sites, and between field sites and mesocosms. The greater the long-term (annual) average dissolution rate, the greater the long-term average Ω_a has to be for a positive rate of NCC to be achieved over long timescales (years–decades) (Cyronak et al. 2013; Eyre et al. 2014). The fact that the x-intercept from the mesocosm studies is lower than that from field studies might reflect lower dissolution rates in mesocosms because they do not replicate the environments and biota where dissolution is likely to be most active, i.e., in the sediments and the reef framework. If this interpretation is correct, it would follow that the dissolution rate is much higher at the reef in Japan studied by Ohde and van Woesik (1999) and much lower at Lady Eliot Island Reef studied by Shaw et al. (2012).

It is also interesting to compare the slopes of the NCC versus Ω_a relationships. It is useful to apply a normalization before attempting such a comparison because the absolute rate varies considerably due to differences in abundance and community composition of the calcifiers found at each study site, and due to the differences in carbonate framework and sediment environments and biota responsible for dissolution. Borrowing from the literature on laboratory experiments with corals, a commonly used normalization is to express the rates as a percentage of the rate at some reference saturation state, such as the pre-industrial value 4.6 (Langdon and Atkinson 2005; Kleypas and Langdon 2006; Chan and Connolly 2013). In a meta-analysis of 30 laboratory studies, Chan and Connolly (2013) found that

Fig. 5 The paths over which water is assumed to have flowed from the reef edge to the sampling point on **a** December 7, **b** December 8, **c** May 21, **d** May 22, and **e** May 23, indicated with *colors* which correspond to the hour during which the transect was sampled, according to the key. The *black loop* indicates the reef edge, *black points* indicate the points on the reef at which water samples were collected. The *arrows* indicate northerly direction. The length of one transect on May 21 (**c**) is indicated for scale



the average response of corals was a 15 ± 8 % decrease in calcification per unit change in Ω_a . In this study, NCC was found to be considerably more sensitive to Ω_a with a 68 ± 33 % change in calcification per unit change in Ω_a (Table 5). The sensitivity to Ω_a varies from a low of

30 ± 11 % to a high of 85 ± 8 % per unit change in Ω_a in field studies (Table 5). The fact that coral reef communities in nature seem to be more sensitive to a change in Ω_a than individual corals in a laboratory setting (where carbonate sand or framework are absent) is consistent with the finding

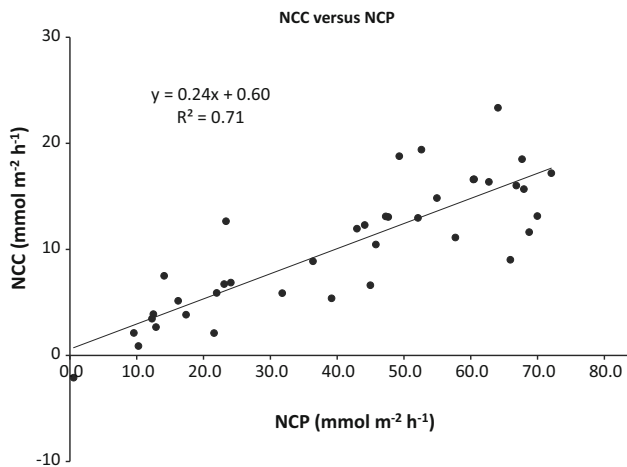


Fig. 6 Correlation between net community calcification (NCC) and net community productivity (NCP) ($p < 0.0001$). See Table 4 for regression data and statistics

that dissolution may be more sensitive than calcification to declining Ω_a (Cyronak et al. 2013; Eyre et al. 2014). It is worth noting that mesocosms seem to capture an intermediate response with sensitivities in the range of 27–34 % per unit change in Ω_a .

There are several possible reasons that coral reef communities in nature might exhibit a higher sensitivity to a change in Ω_a than in laboratory and mesocosm studies. One obvious reason is that laboratory studies are generally performed under optimal or near-optimal light and temperature conditions. It is quite possible that corals in the field experiencing sub-optimal environmental conditions will be less able to cope with the additional stress of reduced pH and will therefore show a greater sensitivity to a reduction in Ω_a . A second reason could be that food

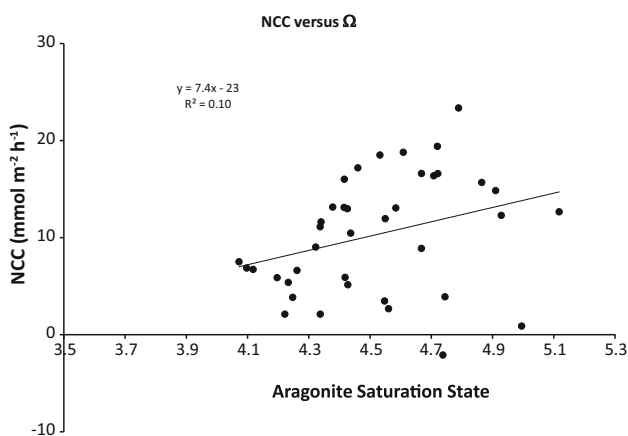


Fig. 7 Correlation between net community calcification (NCC) and aragonite saturation state (Ω_a) ($p = 0.05$). See Table 4 for regression data and statistics

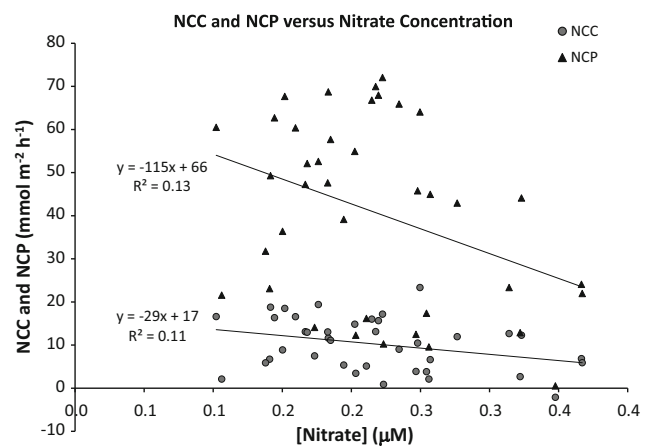


Fig. 8 Net community calcification (NCC, circles) and net community productivity (NCP, triangles) both correlate weakly with nitrate concentration [NO_3^{2-}] but the correlations are significant ($p = 0.05$ and $p = 0.04$, respectively)

scarcity and interactions with other species (competition, predator–prey, disease) could reduce a coral’s energy reserves and hence its ability to devote the extra energy needed to elevate pH from a lower baseline at the site of calcification. Thirdly, the differences in sensitivity of NCC to Ω_a may be reflecting the limited ability of laboratory and mesocosm experiments to replicate the environments and biota involved in dissolution, and thus the limited ability of those experiments to capture the full sensitivity of dissolution to Ω_a that is exhibited in the field (Cyronak et al. 2013; Eyre et al. 2014). The fact that laboratory and mesocosm studies may be underestimating both the sensitivity to a reduction in Ω_a and the critical Ω_a below which reef framework starts to dissolve is cause for concern as this means that the threat of OA may be more pressing than we previously thought.

Reconciling the two explanations

While it is reasonable that both the x-intercept and sensitivity of the NCC– Ω_a relationship are higher in nature than in the laboratory and in mesocosms for the reasons given above, it is also likely that some of the difference may be explained by the fact that in field studies it is easy to confound the effects of Ω_a on NCC with other factors that control NCC. It is likely that the truth lies somewhere between the two explanations offered above. The x-intercept and slope in natural coral reef communities may be greater than those found in laboratory and mesocosm studies because of poorly replicated community structure lacking sufficient representation of sand and carbonate framework involved in dissolution. On the other hand, some of the extremely high x-intercepts and steep slopes

Table 3 Average daytime net community calcification (NCC) and net community productivity (NCP) rates ($\text{mmol m}^{-2} \text{h}^{-1}$) and environmental data, including percent calcifier cover (%CC), aragonite saturation state (Ω_a), and photosynthetically active radiation (PAR, $\mu\text{E m}^{-2} \text{s}^{-1}$) for several field and mesocosm studies

Reference	%CC	Season/treatment	Ω_a	T on Reef (°C)	Daily Integrated PAR ($\text{E m}^{-2} \text{d}^{-1}$)	Daytime NCC $\text{mmol m}^{-2} \text{h}^{-1}$	Daytime NCP $\text{mmol m}^{-2} \text{h}^{-1}$
This study	61	December 2010	4.62	30	30	8	21
	61	May 2011	4.50	28	37	11	44
Falter et al. (2012)	70	Winter 2009	4.17	24.7	20.3	18	N/A
	70	Summer 2008	3.53	23.7	40.9	16	N/A
Shaw et al. (2012)	40	Feb 2010	4.09	28.0	N/A	9	N/A
	40	April 2010	4.40	26.6	N/A	10	N/A
	40	July 2010	3.99	23.2	N/A	11	N/A
Shamberger et al. (2011)	25	Feb 2010	2.71	23	28.4	15.7	3.3
	25	June 2008, August 2009	2.87	26.3	39.0	9.9	13.41
Bates et al. (2010)	21	Jan–April 2003	3.08	21	N/A	5.3	N/A
	21	July–August 2003	3.35	29	N/A	4.8	N/A
	21	September–December 2002	3.26	24	N/A	2.4	N/A
Silverman et al. (2007a, b)	10	Winter 2000–2002	3.98	21.8	17.7	2.3	14
	10	Summer 2000–2002	3.97	24.2	20.6	2.5	17
Yates and Halley (2006)	10	Feb 2000	3.00	26.18	40.4	0.48	3.52
	22	Feb 2000	3.05	25.43	49.4	1.73	7.79
	10	July 2001	2.40	27.73	43.5	0.69	−0.23
Watanabe et al. (2006)	16	April 2000	3.78	28.3	N/A	6.0	−2.08
	16	September 2000	3.83	29.4	32.4	6.1	N/A
Ohde and van Woesik (1999)	36	October/September 1993–1995	5.38	30.38	N/A	7.07	9.98
	36	June/July 1994	5.80	31.30	N/A	12	16
Gattuso et al. (1997)	15	July 16–17 1992	3.61	27.3	35.6	3.25	15
Gattuso et al. (1996)	29	July, August 1992, Austral winter	5.38	27.1	43.2	13.5	70
	40	December 1993, Austral summer	5.04	27.2	43.2	17.5	100
Andersson et al. (2009)	25	Control June 2006	3.33	27.5	N/A	6.033	N/A
	25	Treatment June 2006	1.85	27.43	N/A	1.6	N/A
Langdon and Atkinson (2005)	100	Winter	3.01	23.8	15.4	15.4	23
	100	Winter	2.27	23.8	17.9	12	32
	100	Winter	1.65	24.4	18.4	3	35
	100	Summer	3.00	27.3	26.3	16	45
	100	Summer	1.80	27.3	24.6	9	55
Langdon et al. (2000)	40	Two long experiments 1995–1998	1.60	26.5	N/A	0.4	N/A
	40	Last glacial maximum pCO_2	3.10	26.5	N/A	3	N/A
	40	Present day pCO_2	5.20	26.5	N/A	10	N/A
Langdon (2002)	40	Present day pCO_2	3.35	26.5	N/A	4.3	N/A
	40	$2 \times$ present day pCO_2	2.05	26.5	N/A	2.7	N/A

See ESM Table S2 for details on each data source

from field studies may be artifacts produced by the confounding effects of NCP and light on NCC (Falter et al. 2012). Resolving a clearer understanding of the NCC– Ω_a

relationship requires additional estimates of NCC along with thorough characterization of the full suite of environmental conditions: NCP, Ω_a , temperature, PAR, percent

Table 4 Regressions between net community calcification (NCC) and net community productivity (NCP), and temperature, photosynthetically available radiation (PAR), aragonite saturation state (Ω_a), and nitrate concentration ($[\text{NO}_3^{2-}]$)

	p	r^2	Slope	Slope error	p	r^2	Slope	Slope error
	Temperature				PAR			
NCC	0.7	0.003	−0.5	1	0.1	0.06	0.003	0.002
NCP	0.1	0.06	−8	5	0.7	0.004	0.003	0.007
	Ω_a				$[\text{NO}_3^{2-}]$			
NCC	0.05	0.10	7	4	0.04	0.11	−29	13
NCP	0.5	0.01	8	13	0.02	0.13	−115	48
	p		r^2		Slope		Slope error	
NCC versus NCP	1e−11		0.71		0.24		0.02	
Ω_a versus PAR	7e−06		0.4		0.0003		6e−05	

The regressions are weak (low r^2) and all are insignificant ($p > 0.05$) except for NCC versus Ω_a and NCC and NCP versus $[\text{NO}_3^{2-}]$

Table 5 Regression data for this study and several previously published studies

	Slope	y-intercept	x-intercept	NCC at $\Omega_a = 4.6$	% $\Delta\text{NCC}_{4.6}/\Delta\Omega_a$
<i>Field studies</i>					
This study	7.37	−23	3.1 ± 2.7	10.9	68 ± 33
Falter et al. (2012)	20.7	−57.6	2.8 ± 1.3	37.6	55 ± 16
Shaw et al. (2012)	3.4	−4.2	1.2 ± 1.6	11.4	30 ± 11
Shamberger et al. (2011)	10.2	−17.3	1.7 ± 0.8	29.6	35 ± 8
Silverman et al. (2007b)	4.32	−14.8	3.4 ± 0.5	5.1	85 ± 8
Ohde and van Woesik (1999) ^a	8.5	−40.9	4.9 ± 0.3	−1.8	—
Average			2.9 ± 0.5		
<i>Mesocosm studies</i>					
Andersson et al. (2009)	3.4	−5.3	1.1 ± 0.4	10.3	29 ± 4
Langdon and Atkinson (2005) ^b	7.8	−7.3	0.9 ± 0.6	28.7	27 ± 6
Kleypas and Langdon (2006)	34.1	−58.7	1.7 ± 0.3	98.2	34 ± 3
LeClercq et al. (2002)	1.20E−02	9.80E−02	−8.2	0.2	7.8
Average ^c			1.2 ± 0.1		

The x-intercept is the aragonite saturation state (Ω_a) at which net communication calcification equals zero (NCC = 0). The percent change (Δ) in NCC per unit change in Ω_a is also listed, where the NCC rates are expressed as a percentage of the rate at the pre-industrial Ω_a value of 4.6

^a Normalized pre-industrial sensitivity not calculated because 4.6 is outside the range of saturation states observed on this reef

^b Only uses the pre-nutrient addition data

^c Excluded the x-intercept for LeClercq et al. (2002) because a saturation state below zero is not realistic

calcifier cover, and nutrient levels. With broader geographic and temporal coverage, we will then be able to average out the short-term confounding factors and capture a general relationship, with predictive power to understand the impact of long-term OA on NCC.

Acknowledgments We would like to thank Craig Marquette, James Churchill, Pedro De La Torre, William Decarvalho, Jessica Masterman, Luke Mays, Elizabeth Bonk and Rebecca Belastock for assisting

in sampling and analysis of samples. We would also like to thank Tom Farrar for providing files of surface irradiance and wind speed. This research was supported by Award No. USA 00002 and KSA 00011 to K. Huguen, D. McCorkle, and S. Lentz made by King Abdullah University of Science and Technology. This material is based upon work supported under a National Science Foundation Graduate Research Fellowship. Any opinions, findings, conclusions or recommendations expressed in this publication are those of the authors and do not necessarily reflect the views of the National Science Foundation.

References

- Adey WH (1998) Coral reefs: algal structured and mediated ecosystems in shallow, turbulent, alkaline waters. *J Phycol* 34:393–406
- Albright R, Langdon C, Anthony K (2013) Dynamics of seawater carbonate chemistry, production, and calcification of a coral reef flat, central Great Barrier Reef. *Biogeosci Discuss* 10:7641–7676
- Allemand D, Ferrier-Pages C, Furla P, Houlbreque F, Puverel S, Reynaud S, Tambutte E, Tambutte S, Zoccola D (2004) Biomineralisation in reef-building corals: from molecular mechanisms to environmental control. *C R Palevol* 3:453–467
- Andersson AJ, Gledhill D (2013) Ocean acidification and coral reefs: effects on breakdown, dissolution, and net ecosystem calcification. *Ann Rev Mar Sci* 5:321–348
- Andersson AJ, Kuffner IB, Mackenzie FT, Jokiel PL, Rodgers KS, Tan A (2009) Net loss of CaCO₃ from a subtropical calcifying community due to seawater acidification: mesocosm-scale experimental evidence. *Biogeosciences* 6:1811–1823
- Anthony KRN, Kline DI, Diaz-Pulido G, Dove S, Hoegh-Guldberg O (2008) Ocean acidification causes bleaching and productivity loss in coral reef builders. *Proc Natl Acad Sci USA* 105:17442–17446
- Apprill A, Rappe MS (2011) Response of the microbial community to coral spawning in lagoon and reef flat environments of Hawaii, USA. *Aquat Microb Ecol* 62:251–266
- Atkinson MJ, Cuet P (2008) Possible effects of ocean acidification on coral reef biogeochemistry: topics for research. *Mar Ecol Prog Ser* 373:249–256
- Atkinson M, Falter J (2003) Coral reefs. In: Black KD, Shimmield GB (eds) *Biogeochemistry of marine systems*. CRC Press, Boca Raton
- Atkinson M, Smith S (1983) C:N: P ratios of benthic marine plants. *Limnol Oceanogr* 23:568–574
- Baker KS, Frouin R (1987) Relation between photosynthetically available radiation and total insolation at the surface of the ocean under clear skies. *Limnol Oceanogr* 32:1370–1377
- Barnes DJ (1982) Light response curve for calcification in the staghorn coral, *Acropora acuminata*. *Comp Biochem Physiol A Physiol* 73:41–45
- Bates NR, Amat A, Andersson AJ (2010) Feedbacks and responses of coral calcification on the Bermuda reef system to seasonal changes in biological processes and ocean acidification. *Biogeosciences* 7:2509–2530
- Birrell CL, McCook LJ, Willis BL, Diaz-Pulido GA (2008) Effects of benthic algae on the replenishment of corals and the implications for the resilience of coral reefs. *Oceanogr Mar Biol Annu Rev* 46:25–63
- Bischoff WD, Mackenzie FT, Bishop FC (1987) Stabilities of synthetic magnesian calcites in aqueous solution: comparison with biogenic materials. *Geochim Cosmochim Acta* 51:1413–1423
- Bjork M, Mohammad SM, Bjorklund M, Semesi A (1995) Coralline algae, important coral reef builders threatened by pollution. *Ambio* 24:502–505
- Chalker BE, Taylor DL (1975) Light-enhanced calcification, and role of oxidative-phosphorylation on calcification of coral *Acropora cervicornis*. *Proc R Soc Lond B Biol Sci* 190:323–331
- Chan NCS, Connolly SR (2013) Sensitivity of coral calcification to ocean acidification: a meta-analysis. *Glob Chang Biol* 19:282–290
- Chisholm JRM (2000) Calcification by crustose coralline algae on the northern Great Barrier Reef, Australia. *Limnol Oceanogr* 45:1476–1484
- Cohen AL, Holcomb M (2009) Why corals care about ocean acidification: uncovering the mechanism. *Oceanography* 22:118–127
- Cyronak T, Santos IR, Eyre BD (2013) Permeable coral reef sediment dissolution driven by elevated pCO₂ and pore water advection. *Geophys Res Lett* 40:4876–4881
- Dickson AG, Millero FJ (1987) A comparison of the equilibrium constants for the dissociation of carbonic acid in seawater media. *Deep Sea Res A* 34:1733–1743
- Donnan DW, Moore PG (2003) Introduction. *Aquat Conserv* 13:S1–S3
- Eyre B, Andersson AJ, Cyronak T (2014) Benthic coral reef calcium carbonate dissolution in an acidifying ocean. *Nat Clim Chang* 4:969–976
- Erez J (1990) On the importance of food sources in coral-reef ecosystems. In: Dubinsky Z (ed) *Ecosystems of the world: coral reefs*. Elsevier, Amsterdam, pp 411–418
- Falter JL, Lowe RJ, Atkinson MJ, Cuet P (2012) Seasonal coupling and de-coupling of net calcification rates from coral reef metabolism and carbonate chemistry at Ningaloo Reef, Western Australia. *J Geophys Res Oceans* 117:C05003
- Falter JL, Lowe RJ, Zhang Z, McCulloch M (2013) Physical and biological controls on the carbonate chemistry of coral reef waters: effects of metabolism, wave forcing, sea level, and geomorphology. *PLoS One* 8:e53303
- Falter JL, Lowe RJ, Atkinson MJ, Monismith SG, Schar DW (2008) Continuous measurements of net production over a shallow reef community using a modified Eulerian approach. *J Geophys Res Oceans* 113:C07035
- Foster MS (2001) Rhodoliths: between rocks and soft places. *J Phycol* 37:659–667
- Frankignoulle M, Gattuso JP, Biondo R, Bourge I, CopinMontegut G, Pichon M (1996) Carbon fluxes in coral reefs. 2. Eulerian study of inorganic carbon dynamics and measurement of air-sea CO₂ exchanges. *Mar Ecol Prog Ser* 145:123–132
- Gattuso JP, Allemand D, Frankignoulle M (1999) Photosynthesis and calcification at cellular, organismal and community levels in coral reefs: a review on interactions and control by carbonate chemistry. *Am Zool* 39:160–183
- Gattuso JP, Pichon M, Delesalle B, Canon C, Frankignoulle M (1996) Carbon fluxes in coral reefs. 1. Lagrangian measurement of community metabolism and resulting air-sea CO₂ disequilibrium. *Mar Ecol Prog Ser* 145:109–121
- Gattuso JP, Payri CE, Pichon M, Delesalle B, Frankignoulle M (1997) Primary production, calcification, and air-sea CO₂ fluxes of a macroalgal-dominated coral reef community (Moorea, French Polynesia). *J Phycol* 33:729–738
- Goreau TF, Goreau NI (1959) The physiology of skeleton formation in corals. II. Calcium deposition by hermatypic corals under various conditions in the reef. *Biol Bull* 117:239–250
- Grigg RW (1982) Darwin point: a threshold for atoll formation. *Coral Reefs* 1:29–34
- Houlbreque F, Tambutte E, Ferrier-Pages C (2003) Effect of zooplankton availability on the rates of photosynthesis, and tissue and skeletal growth in the scleractinian coral *Stylophora pistillata*. *J Exp Mar Biol Ecol* 296:145–166
- Jokiel PL, Rodgers KS, Kuffner IB, Andersson AJ, Cox EF, Mackenzie FT (2008) Ocean acidification and calcifying reef organisms: a mesocosm investigation. *Coral Reefs* 27:473–483
- Kinsey DW (1983) Standards of performance in coral reef primary production and carbon turnover. In: Barnes DJ (ed) *Perspectives on coral reefs*. Australian Institute of Marine Science, Townsville, pp 209–220
- Kinsey DW (1985) Metabolism, calcification and carbon production. In: *Proceedings of 5th international coral reef symposium*, vol. 4, pp 505–526
- Kleypas JA, Langdon C (2006) Coral reefs and changing seawater carbonate chemistry. In: Phinney J, Hoegh-Guldberg O, Kleypas J, Skirving W, Strong A (eds) *Coral reefs and climate change: science and management*. American Geophysical Union, Washington, pp 73–110

- Kleypas JA, McManus JW, Menez LAB (1999) Environmental limits to coral reef development: where do we draw the line? *Am Zool* 39:146–159
- Kleypas JA, Feely RA, Fabry JV, Langdon C, Sabine CL, Robbins LL (2006) Impacts of ocean acidification on coral reefs and other marine calcifiers: a guide for future research, report of a workshop held 18–20 April 2005, St. Petersburg, FL, sponsored by NSF, NOAA, and the US Geological Survey, 88
- Kuffner IB, Andersson AJ, Jokiel PL, Rodgers KS, Mackenzie FT (2008) Decreased abundance of crustose coralline algae due to ocean acidification. *Nat Geosci* 1:114–117
- Langdon C (2002) Review of experimental evidence for effects of CO₂ on calcification of reef builders. In: Proceedings of 9th international coral reef symposium, vol. 2, pp 1091–1098
- Langdon C, Atkinson MJ (2005) Effect of elevated pCO₂ on photosynthesis and calcification of corals and interactions with seasonal change in temperature/irradiance and nutrient enrichment. *J Geophys Res Oceans* 110:1–16
- Langdon C, Gattuso JP, Andersson AJ (2010) Measurements of calcification and dissolution of benthic organisms and communities. In: Riebesell U, Fabry VJ, Hansson L, Gattuso JP (eds) Guide to best practices for ocean acidification research and data reporting. Publications Office of the European Union, Luxembourg, pp 213–232
- Langdon C, Takahashi T, Sweeney C, Chipman D, Goddard J, Marubini F, Aceves H, Barnett H, Atkinson MJ (2000) Effect of calcium carbonate saturation state on the calcification rate of an experimental coral reef. *Glob Biogeochem Cycles* 14:639–654
- Leclercq N, Gattuso JP, Jaubert J (2000) CO₂ partial pressure controls the calcification rate of a coral community. *Glob Chang Biol* 6:329–334
- Leclercq N, Gattuso JP, Jaubert J (2002) Primary production, respiration, and calcification of a coral reef mesocosm under increased CO₂ partial pressure. *Limnol Oceanogr* 47:558–564
- Martin S, Gattuso JP (2009) Response of Mediterranean coralline algae to ocean acidification and elevated temperature. *Glob Chang Biol* 15:2089–2100
- Marubini F, Davies PS (1996) Nitrate increases zooxanthellae population density and reduces skeletogenesis in corals. *Mar Biol* 127:319–328
- Marubini F, Atkinson M (1999) Effects of lowered pH and elevated nitrate on coral calcification. *Mar Ecol Prog Ser* 188:117–121
- Marubini F, Barnett H, Langdon C, Atkinson MJ (2001) Dependence of calcification on light and carbonate ion concentration for the hermatypic coral *Porites compressa*. *Mar Ecol Prog Ser* 220:153–162
- McCulloch M, Falter J, Trotter J, Montagna P (2012) Coral resilience to ocean acidification and global warming through pH up-regulation. *Nat Clim Chang* 2:623–627
- McMahon A, Santos IR, Cyronak T, Eyre BD (2013) Hysteresis between coral reef calcification and the seawater aragonite saturation state. *Geophys Res Lett* 40:4675–4679
- Mehrbach C, Culbertson CH, Hawley JE, Pytkowicz RM (1973) Measurement of apparent dissociation constants of carbonic acid in seawater at atmospheric pressure. *Limnol Oceanogr* 18:897–907
- Morse DE, Morse ANC, Raimondi PT, Hooker N (1994) Morphogen-based chemical flypaper for *Agaricia humilis* coral larvae. *Biol Bull* 186:172–181
- Morse JW, Andersson AJ, Mackenzie FT (2006) Initial responses of carbonate-rich shelf sediments to rising atmospheric pCO₂ and “ocean acidification”: role of high Mg-calcites. *Geochim Cosmochim Acta* 70:5814–5830
- Mucci A (1983) The solubility of calcite and aragonite in seawater at various salinities, temperatures, and one atmosphere total pressure. *Am J Sci* 283:780–799
- Muscantine L, Goiran C, Land L, Jaubert J, Cuif JP, Allemand D (2005) Stable isotopes ($\delta^{13}\text{C}$ and $\delta^{15}\text{N}$) of organic matrix from coral skeleton. *Proc Natl Acad Sci USA* 102:1525–1530
- Odum HT (1956) Primary production in flowing waters. *Limnol Oceanogr* 1:102–117
- Ohde S, van Woesik R (1999) Carbon dioxide flux and metabolic processes of a coral reef, Okinawa. *Bull Mar Sci* 6:559–576
- Pandolfi JM, Connolly SR, Marshall DJ, Cohen AL (2011) Projecting coral reef futures under global warming and ocean acidification. *Science* 333:418–422
- Pierrot DEL, Wallace DWR (2006) MS excel program developed for CO₂ system calculations. ORNL/CDIAC-105a
- Ribes M, Coma R, Atkinson MJ, Kinzie RA (2003) Particle removal by coral reef communities: picoplankton is a major source of nitrogen. *Mar Ecol Prog Ser* 257:13–23
- Shamberger KEF, Feely RA, Sabine CL, Atkinson MJ, DeCarlo EH, Mackenzie FT, Drupp PS, Butterfield DA (2011) Calcification and organic production on a Hawaiian coral reef. *Mar Chem* 127:64–75
- Shaw EC, McNeil BI, Tilbrook B (2012) Impacts of ocean acidification in naturally variable coral reef flat ecosystems. *J Geophys Res Oceans* 117:C03038
- Silverman J, Lazar B, Erez J (2007a) Community metabolism of a coral reef exposed to naturally varying dissolved inorganic nutrient loads. *Biogeochemistry* 84:67–82
- Silverman J, Lazar B, Erez J (2007b) Effect of aragonite saturation, temperature, and nutrients on the community calcification rate of a coral reef. *J Geophys Res Oceans* 112:C05004
- Silverman J, Kline D, Johnson L, Rivlin T, Schneider K, Erez J, Lazar B, Caldeira K (2012) Carbon turnover rates in the One Tree Island reef: a 40-year perspective. *J Geophys Res* 117:G03023
- Stoddart DR (1969) Ecology and morphology of recent coral reefs. *Biol Rev* 44:433–498
- Sweeney C, Gloor E, Jacobson AR, Key RM, McKinley G, Sarmiento JL, Wanninkhof R (2007) Constraining global air-sea gas exchange for CO₂ with recent bomb C-14 measurements. *Glob Biogeochem Cycles* 21:GB2015
- Venn A, Tambutté E, Holcomb M, Allemand D, Tambutté S (2011) Live tissue imaging shows reef corals elevate pH under their calcifying tissue relative to seawater. *PLoS One* 6:e20013
- Venn A, Tambutte E, Holcomb M, Laurent J, Allemand D, Tambutte S (2013) Impact of seawater acidification on pH at tissue-skeleton interface and calcification in reef corals. *Proc Natl Acad Sci USA* 110:1634–1639
- Venti A, Andersson A, Langdon C (2014) Multiple driving factors explain spatial and temporal variability in coral calcification rates on the Bermuda platform. *Coral Reefs* 33:979–997
- Wainwright SA (1963) Skeletal organization in the coral, *Pocillopora damicornis*. *Q J Microsc Sci* 3:169–183
- Wanninkhof R (1992) Relationship between wind speed and gas exchange over the ocean. *J Geophys Res Oceans* 97:7373–7382
- Watanabe A, Kayanne H, Hata H, Kudo S, Nozaki K, Kato K, Negishi A, Ikeda Y, Yamano H (2006) Analysis of the seawater CO₂ system in the barrier reef-lagoon system of Palau using total alkalinity-dissolved inorganic carbon diagrams. *Limnol Oceanogr* 51:1614–1628
- Yates KK, Halley RB (2003) Measuring coral reef community metabolism using new benthic chamber technology. *Coral Reefs* 22:247–255
- Yates KK, Halley RB (2006) CO₃²⁻ concentration and pCO₂ thresholds for calcification and dissolution on the Molokai reef flat, Hawaii. *Biogeosciences* 3:357–369
- Zhang Z, Falter J, Lowe R, Ivey G (2012) The combined influence of hydrodynamic forcing and calcification on the spatial distribution of alkalinity in a coral reef system. *J Geophys Res Oceans* 117:C04034